



# Porous aluminum oxide insulation materials tested in space mission

Péter Ádám<sup>1</sup> · Levente Dudás<sup>2</sup> · Ottó Temesi<sup>3</sup> · András Nagy<sup>4</sup> · Katalin Sinkó<sup>1</sup>

Received: 21 March 2022 / Revised: 2 September 2022 / Accepted: 2 September 2022 / Published online: 27 September 2022  
© The Author(s) 2022

## Abstract

The eventual aim of this research work was to develop a new low-cost synthesis route to produce ultralight aluminum oxide ceramic fibers for high temperature insulation. This paper mainly focuses on the application of  $\text{Al}_2\text{O}_3$  fibers as insulation materials in space vehicles. The study extended to check the fibers during the launch and in the conditions of space by a satellite test. The materials were monitored by thermo-vacuum and vibration tests before the launch. The long-term stability, the daily maximum and minimum temperature, and the temperature fluctuation were investigated in the satellite test. The data derived from satellite was collected in about 9 months. The other focus of this study was the characterization of fibers at high temperature.  $\text{Al}_2\text{O}_3$  fibers were prepared by a new solution method and electrospinning technique. The developed  $\text{Al}_2\text{O}_3$  fibers can be characterized by  $0.035\text{--}0.037 \text{ W}\cdot\text{mK}^{-1}$  thermal conductivity, excellent heat resistance (up to  $1600 \text{ }^\circ\text{C}$ ), and good flexibility.

**Keywords** Satellite test · Aluminum oxide · Insulation · Porous systems

## 1 Introduction

Space missions require materials that can preserve functional integrity under extreme conditions of heat, impact and radiation. The main requirements for space insulation materials are light weight, very low heat conductivity, and outstanding thermal stability. The external tank needs some insulation to maintain the cryogenic fuels, liquid hydrogen, and liquid oxygen as well as to provide additional structural integrity through launch and after release from the orbiter. The extreme thermal conditions in space depend on the type of orbit and on the satellite configuration. During orbital phases around the earth, spacecraft materials and structures are subjected to outside temperatures varying between approximately  $-180 \text{ }^\circ\text{C}$  to  $+180 \text{ }^\circ\text{C}$ . The temperature

very quickly changes between these values owing to the rotating space vehicles, such as satellite. The quick temperature change means bigger challenge for insulation systems together with outside temperature. The protection of cryogenic tanks in launch vehicles already requires more intensive thermal insulation regarding the temperature of the liquid hydrogen ( $-253 \text{ }^\circ\text{C}$ ) and oxygen ( $-183 \text{ }^\circ\text{C}$ ) tanks and the reaction ( $\sim 1000 \text{ }^\circ\text{C}$ ) between oxygen and hydrogen.

The typical thermal insulation materials in space vehicles are [1–5]:

- Polymer foams and their composite

Some examples: Rohacell WF, polymethacrylimide foam can be used up to  $130 \text{ }^\circ\text{C}$  and  $0.7 \text{ MPa}$ ; Eccofoam: polyurethane foam ( $\leq 75 \text{ }^\circ\text{C}$ ); spray-on foam, which a closed cell foam based on polyurethane for insulation of the shuttle fuel tank's outer layers. NASA applied a low-density, rigid, closed-cell polymeric (epoxy) foam. This foam is referred to as a tank insulator.<sup>2</sup> The other system is a composite material made of silicone resins and cork. That can also be applied for insulation of the liquid hydrogen tank [1].

- Porous inorganic materials

✉ Péter Ádám  
adam.peter89@gmail.com

✉ Katalin Sinkó  
sinkokatl@caesar.elte.hu

<sup>1</sup> Eötvös Loránd University, Institute of Chemistry, Budapest H-1117, Hungary

<sup>2</sup> Budapest University of Technology and Economics, Budapest 1111, Hungary

<sup>3</sup> H ION Ltd, Budapest 1221, Hungary

<sup>4</sup> ATL Zrt, Budakalász 2011, Hungary

These materials can be characterized with nanometer scale open pore structure, very low bulk density, and extremely low heat conductivity. Some examples: silica aero- and cryogel products of ASPEN, polymer cross-linked aerogels, polyamide aerogels [2–5]. They are good candidates as isolation materials for hypersonic cryogenic tank.

– Multi-layer-insulation systems (MLI)

MLI provide a lightweight insulation system with a high thermal resistance in vacuum. MLI blankets consist of a number of highly reflecting radiation shields such as silver aluminized Mylar layer or other metallized polymer films covered with gold foil; Kapton foil; and thermal insulation layers such as aerogel layer or fiberglass mat or paper [2–5].

– Fiberglass

Fibrous insulation materials may be pure silica fiberglass or glass fiber reinforced with polymer (epoxy or polyester polymer). One of the most important is the phenolic-impregnated carbon ablators or reinforced carbon–carbon systems ( $\leq 580$  °C) [1–5]. Reinforced carbon–carbon is a composite made by treating graphite fabric that has been pre-impregnated with phenolic resin. The resin polymer is converted to carbon by pyrolysis. In the system of carbon–carbon, silicon carbide is used for reinforcing.

Alumina ceramic fibers are utilized in a wide field of structural and thermal insulation [6], adsorption, and filtering. Alumina fibers are often used as reinforcement materials dispersed in metal, ceramic, or polymer matrix of composite systems [7, 8]. In the aspect of application, aluminum oxide fibers have many advantageous properties: microstructural stability at high temperature, low thermal conductivity, low density, thermal-shock resistance, high corrosion and electrical resistance, and good mechanical strength [9–11].

Many low-cost synthesis routes are known instead of expensive melting techniques to produce aluminum oxide fibers: precipitation [12–15], sol gel [16–18], hydrothermal [19], and CVD methods [20].

In the previous work, we developed a new low-cost synthetic route to prepare  $\text{Al}_2\text{O}_3$  fibers [21]. Aluminum acetate and nitrate are proved to be the best Al starting materials. According to the previous conclusion, the fibers can be drawn from various colloid systems such as sol or gel-like systems. The spinnability favors the anisotropic fine particles or two-dimensional chains. The effective fiber drawing demands gel-like systems rather than course sols. The course sols result in very short and brittle fibers or only spread particles [21.]

In the present work, solution techniques (sol–gel and co-precipitation synthetic routes) were applied for preparing the precursor systems of fiber drawing. The main aim of present

study was to test our fiber materials in space, i.e., in extreme thermal conditions, in between quick temperature changes and high temperatures. Beside the investigation in space, thermo-vacuum and vibration tests, SEM study in the function of temperature and thermal conductivity measurements were carried out to characterize the  $\text{Al}_2\text{O}_3$  fibers.

## 2 Experimental

### 2.1 Synthesis

The starting materials were Al acetate,  $\text{Al}(\text{OOCCH}_3)_2(\text{OH})\cdot\text{H}_2\text{O}$  (Alfa Aesar, 99,8%) and Al nitrate,  $\text{Al}(\text{NO}_3)_3\cdot 9\text{H}_2\text{O}$  (VWR, 99,9%). Aluminium salt was dissolved in distilled water or water-containing alcoholic solvents. Al salt was provided by 80% nitrate and 20% chloride. The molar ratio of precursor solution: ethyl alcohol/ $\text{H}_2\text{O}$ / $\text{NH}_3/\text{Al}^{3+}$  is 20:3:3:1. The basic Al acetate is not soluble in water or alcoholic solvent, it can only be dissolved in strongly acidic ( $\text{pH} \leq 1$ ) or basic ( $\text{pH} > 11$ ) medium. To avoid the basic Al-containing precipitation during the treatment, Al acetate was dissolved in hydrochloride aqueous solution [21]. The molar ratio of precursor solution:  $\text{H}_2\text{O}/\text{HCl}/\text{Al}^{3+}$  is 25:2.25:1. Two types of fiber drawing were applied: electrospinning and solvent spinning. Application of electrospinning leads to formation of best fibers with diameter of 1–10  $\mu\text{m}$  and length of 1–5 cm. The heat treatment of green fibers was performed at 80 and 400 °C. 80 °C is important for the escape of solvent, 400 °C for the development of final bond systems. Slow and graduated heating process is favorably for the longer fibers. The yield was 65–72% of theoretical value.

### 2.2 Characterization

The fiber size and morphology were studied by a FEI Quanta 3D FEG scanning electron microscope (SEM). The SEM images were prepared by the Everhart–Thornley secondary electron detector (ETD), its ultimate resolution is 1–2 nm. Since the conductance of the particles investigated is high enough to remove the electric charge accumulated on the surface, the SEM images were performed in high vacuum without any coverage on the specimen surface. For the best SEM visibility, the particles were deposited on a HOPG (graphite) substrate surface. SEM combined with energy disperse X-ray spectroscopy (EDX) is mainly applied for spatially resolved chemical analysis of monolith samples.

The thermal conductivity of insulation materials such as extremely porous aluminum oxide and randomly woven fiber systems were measured by new facility supported by EURAMET.

*Thermo-vacuum test* has been carried out in Center of Energy Research, Budapest. That is one of the requirements for the launch. A thermal-vacuum test (70 °C, 3 h, 10<sup>-4</sup> Pa) was performed to check the safe operation of the satellite and to detect possible material evaporations (which could damage other satellites in POD). In addition, a cyclic vacuum and cyclic vacuum heating test (4x) was performed simulating the space conditions. In space conditions, the thermal conduction is based on the thermal conduction of metal parts and/or heat radiation due to the vacuum. The applied level of vacuum was 10<sup>-4</sup> Pa, the temperature range covered from - 40 °C to +70 °C, the heating and cooling rate were 6 °C/min, and the dwell time was 15 min. Under the whole testing time the batteries were covered with our test samples. The criterion is that the evaporation and the material weight loss should be below 1% [22]. The reference material was stainless steel plate.

*Vibration test* has been performed in an accredited laboratory of BHE Bonn Hungary Electronics Ltd, Budapest. In the test, the qualification specimens were shaken by 20 G sinusoidal normal, and 65 G random impact vibrating load. Accepted level test: the flying specimen was shake 12 G sinusoidal and 10 G random impact vibration load. It both tests, a scanning vibration test was performed 0–20 kHz frequency to get to know, which is the own vibrating frequency (resonance frequencies) of the satellites. That was very important, because if this frequency is close to the vibrations generated during the rocket launch, there is a high chance that the satellite would be damaged during the launch [22]. Under the whole testing time, the batteries were covered with our test samples. The criterion is, that the evaporation and the material weight loss should be below 1% during the test. The reference material was stainless steel plate.

*Satellite test* has been carried out in the satellite shown in Fig. 1. The four IABP85A IABP85A type, 35.8×27.8 × 7.1 mm sized battery were soldered to a PCB panel

and covered by the copper battery cap. The batteries were charged by six pieces solar cells. The investigated materials were placed around 4 batteries in the satellite. During the mission, the temperature was measured by PTS0603 type thermocouples on five different sides of the batteries. The three tested aluminum oxide thermal insulation materials, and the Kapton foil were integrated to cover the batteries and the thermometers. The thickness of insulation layers was 1 mm regarding 1 mm thickness of Kapton foil. The measured data of the thermometers calibrated with a 75 Ohm reference resistor were recorded by the data processing system, and then transmitted by the Communication System (COM) via the on-board computer (OBC) to the Earth. The communication of data was happened at a maximum frequency of 20 kHz with a transmission power of 100 mW, in the 473.15 MHz band at data rates of 5000 and 1250 bit/s. Regarding the period of ATL-1, i.e., 90–92 min, the days were taken into account on those data could be collected during minimum 4.5 h. Thus, the information can be derived from minimum 3 rotation, i.e., 3 temperature cycles.

### 3 Result and discussion

The Al<sub>2</sub>O<sub>3</sub> fibers with other 2 porous Al<sub>2</sub>O<sub>3</sub> materials were tested in ATL-1 CubeSat mission. The ATL-1 is a double CubeSat size (5 × 5 × 10 cm) satellite (Fig. 1) [23]. The main aim of the ATL-1 mission was to investigate these materials and compare with a Kapton foil used commonly in space missions for thermal insulation. The ATL-1 mission was started at 2019.12.06 when the satellite was delivered to a 390 km high Solar Synchronize Orbital as a payload of Rocket Lab’s Electron rocket from New Zealand.

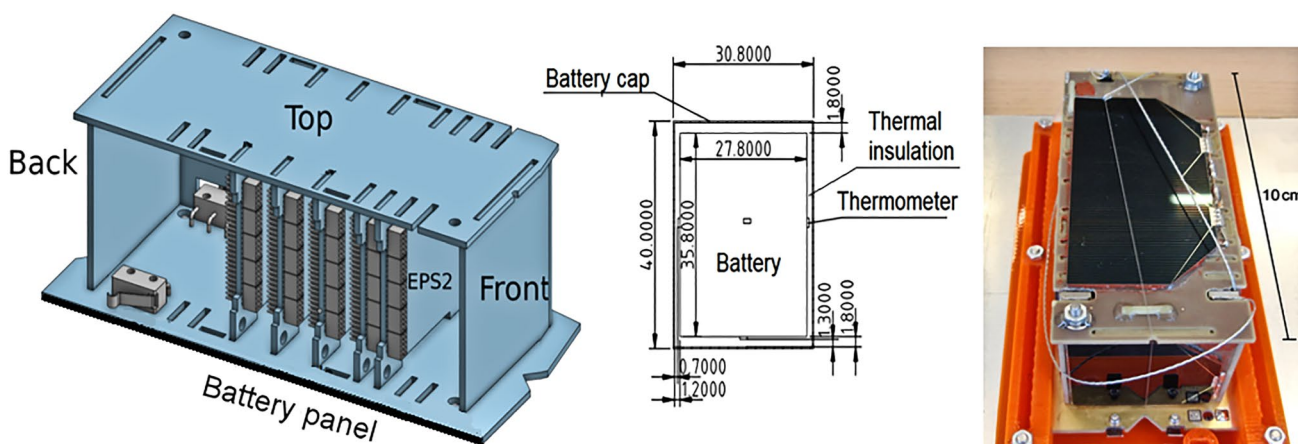


Fig. 1 ATL-1 CubeSat

### 3.1 Preliminary tests of materials for space qualification

Space devices must meet the requirements described by various standards [24]. According to the requirements, the evaporation degree of the satellite may be maximum 1%

weight loss under space conditions, i.e., in vacuum and under vibration (Figs. 2, 3).

At the ATL-1's 360 km high Solar Synchronize Orbital the average temperature was  $-18\text{ }^{\circ}\text{C}$ , due to the distance of the Earth. The electrical system could be operating safety between  $-40\text{ }^{\circ}\text{C}$  and  $+80\text{ }^{\circ}\text{C}$ . The batteries of satellite could

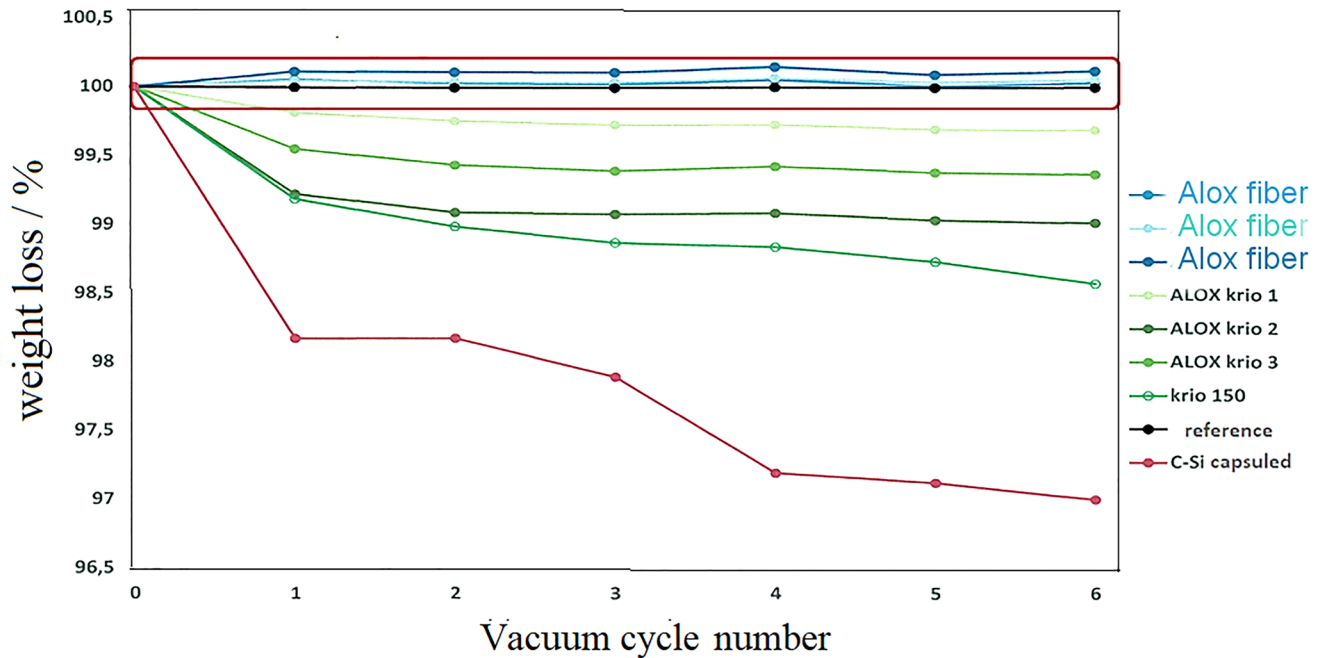


Fig. 2 Weight loss test in vacuum

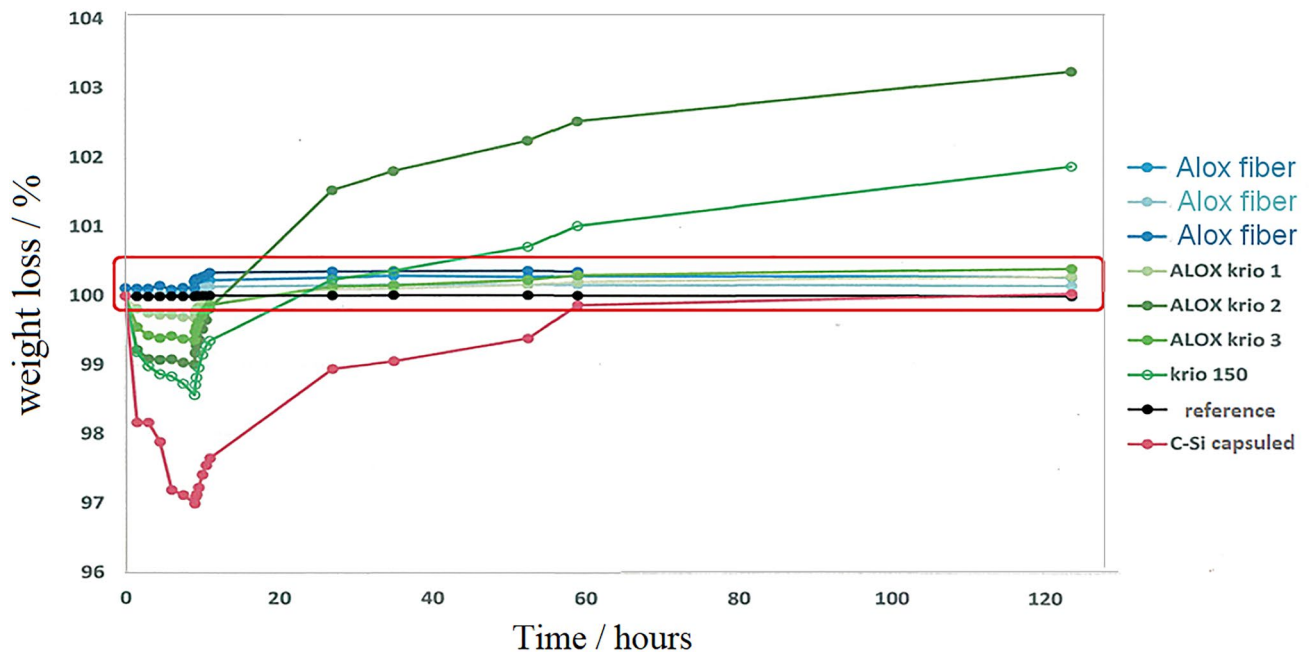


Fig. 3 Weight loss test during vibration

only operate at  $-10\text{ }^{\circ}\text{C}$  and  $+60\text{ }^{\circ}\text{C}$  and could only be charged in the range from  $0\text{ }^{\circ}\text{C}$  to  $+45\text{ }^{\circ}\text{C}$  [22]. These conditions give the importance of thermo-vacuum test (Fig. 2).

The testing and the flying specimen of the ATL-1 satellite were tested on the vibration desk to get to know how the satellite resist of the different vibrating and shaking forces, which can be formed under the launching process. The maximum allowed weight loss is also 1% (Fig. 3).

According to measuring data, our fiber samples fill eminently the requirements, in both cases the weight loss is much less than 1%. That means our fibrous samples and the whole satellite have obtained the space qualification required for the launch.

### 3.2 Analyzing the data derived from satellite

The electric supplies of the ATL-1 satellite were four pieces  $35.8 \times 27.8 \times 7.1$  mm sized battery. The three tested aluminum oxide thermal insulation materials, and the Kapton foil were integrated to cover the batteries and the thermometers. The measuring data were transmitted by the Communication System (COM) via the on-board computer (OBC) to the Earth. Regarding the period of ATL-1, i.e., 90–92 min, the data could be collected during minimum 4.5 h. The information could be collected from minimum 3 rotation, i.e., 3 temperature cycles.

Two databases were created as result of the space mission, one from the telemetry measurements and another from the timed measurements. The final databases are made up of nearly 300,000 data packages, so more than 75,000 measurements were successfully executed and detected at every type of materials. Based on the time stamps, in the case of timed

measurements, which were for a period of 1–1 h, we were able to record a continuous series of several hours/days of measurement data. Telemetry measurements, on the other hand, did not result in a longer data set, nor was the distance between each measurement point equal. For this reason, the results of the two types of measurements were combined and the results of the programmed measurements were supplemented with the results of the telemetry measurement.

Measurement data generated over a longer period are suitable for characterizing the thermal insulation properties and stability of the various tested materials. The insulation character of  $\text{Al}_2\text{O}_3$  fiber has not really changed during near 9 months similar to Kapton foil (Figs. 4, 5, 6). Kapton foil provided for comparison is a typical insulation material for satellite. These results demonstrate the stability of fibers even in extreme conditions. Small reduction in the function of time can be observed only in the maximum and minimum temperature values. The maximum daily temperature fluctuation is plotted to represent the difference between the lowest and highest value of temperature (Fig. 4). The  $\text{Al}_2\text{O}_3$  fibrous insulation used in thickness of 1 mm shows 19–20% smaller temperature fluctuation than Kapton foil. Monitoring the daily minimum and maximum temperature is also very important, because the applied batteries only can operate at the range of  $-10$  to  $+60\text{ }^{\circ}\text{C}$  and can be chargeable at the range of  $0$ – $45\text{ }^{\circ}\text{C}$ . The maximum temperatures meet the requirements in both insulation systems; however, the long-term results of fibers are 12–15% better (Fig. 5). In the minimum temperature, there is larger difference; the data of fibers show 20–60% better values than Kapton foil (Fig. 6). However, both systems meet the operating requirements, but the battery covered with Kapton foil can be chargeable in

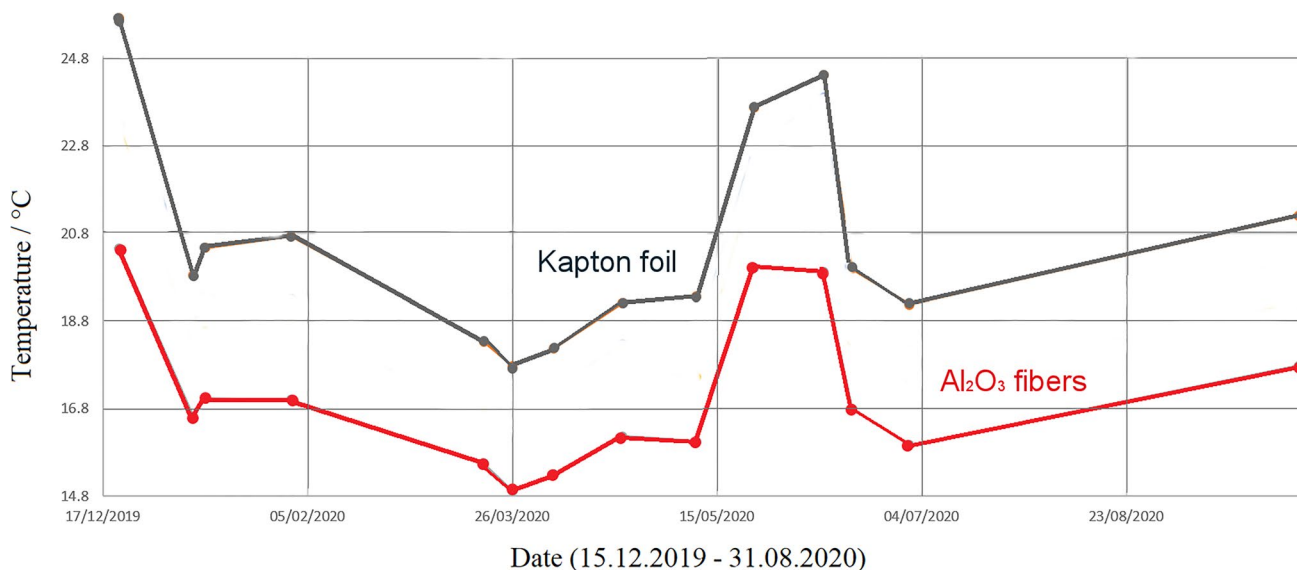
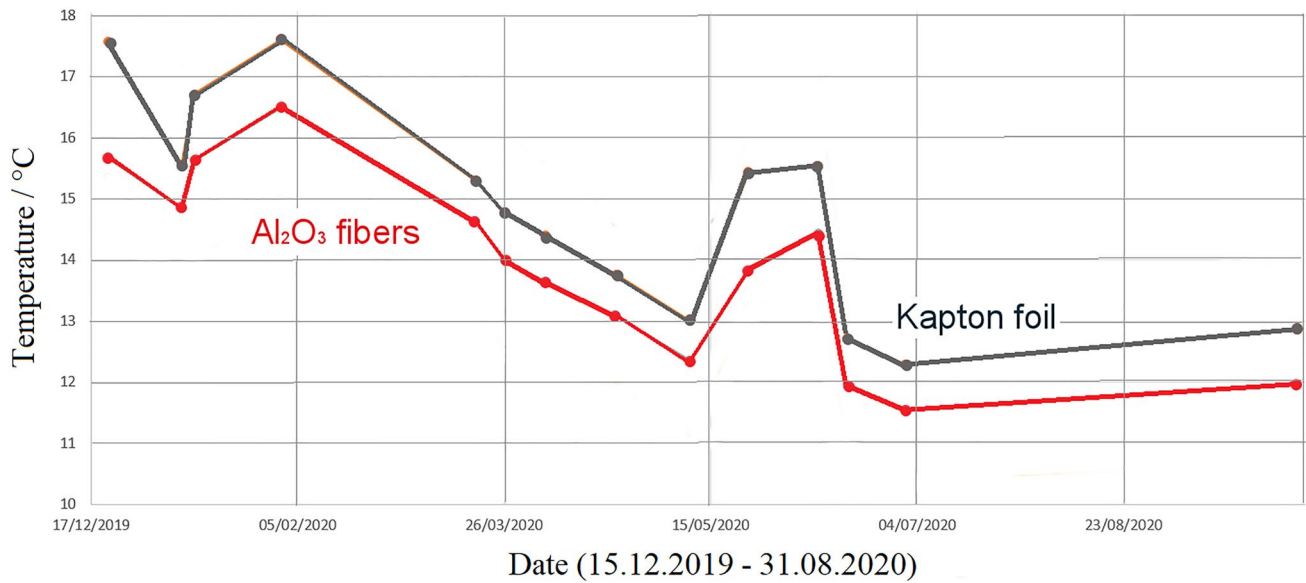
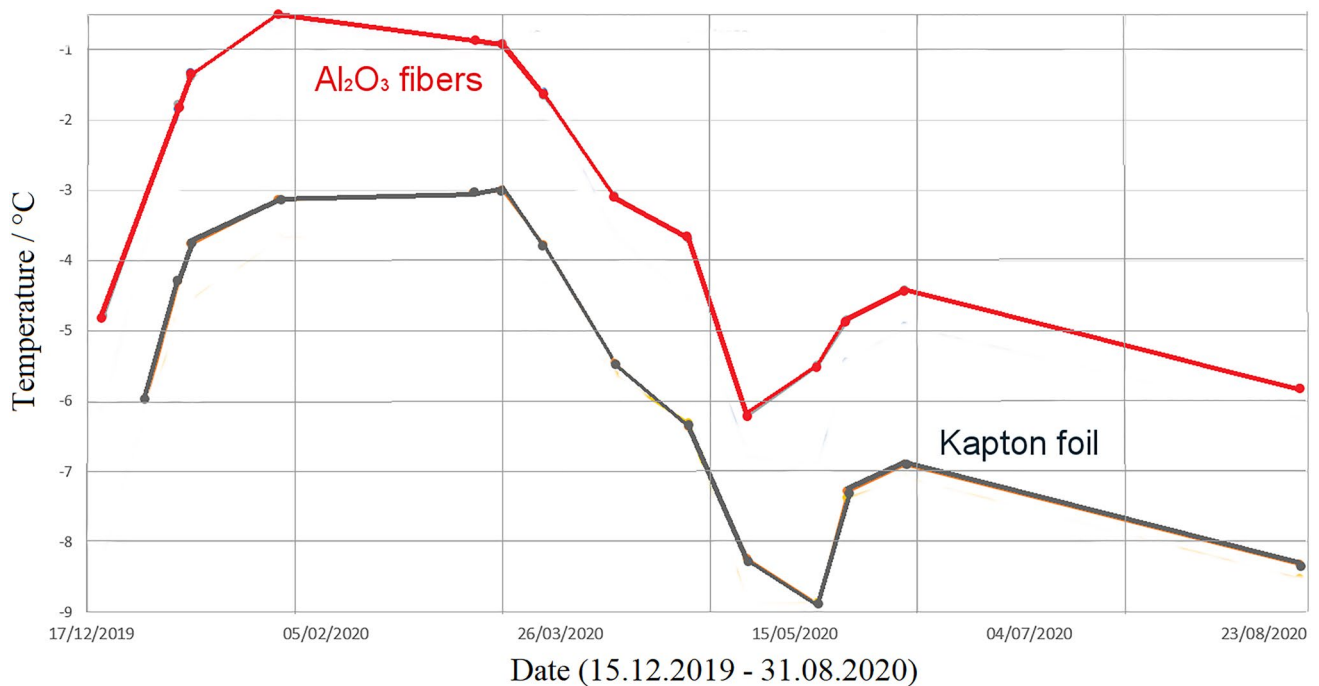


Fig. 4 Daily maximal temperature fluctuation in the time function



**Fig. 5** Changes of daily maximum temperature in the time function



**Fig. 6** Changes of daily minimum temperature in the time function

30–40% shorter time. These results can be achieved using the fibers only in 1 mm layer thickness around the battery. This layer thickness quarantined the reliable comparison with Kapton foil.

Figure 7 represents the homogeneity of insulation systems around the batteries. The temperature curves run closely together in the case of insulation with Al<sub>2</sub>O<sub>3</sub> fibrous layer proving its high homogeneity.

Summarizing the results of the satellite mission, the intensity of thermal insulation ability ( $\lambda$ ) was calculated (Fig. 8). The values were correlated to Kapton foil. The calculated intensity of thermal insulation ability is better with 20–26% per mm than the intensity of Kapton foil. (The thickness of Kapton foil is 1 mm.) This result represents well the previous difference between fibrous and foil insulation materials.

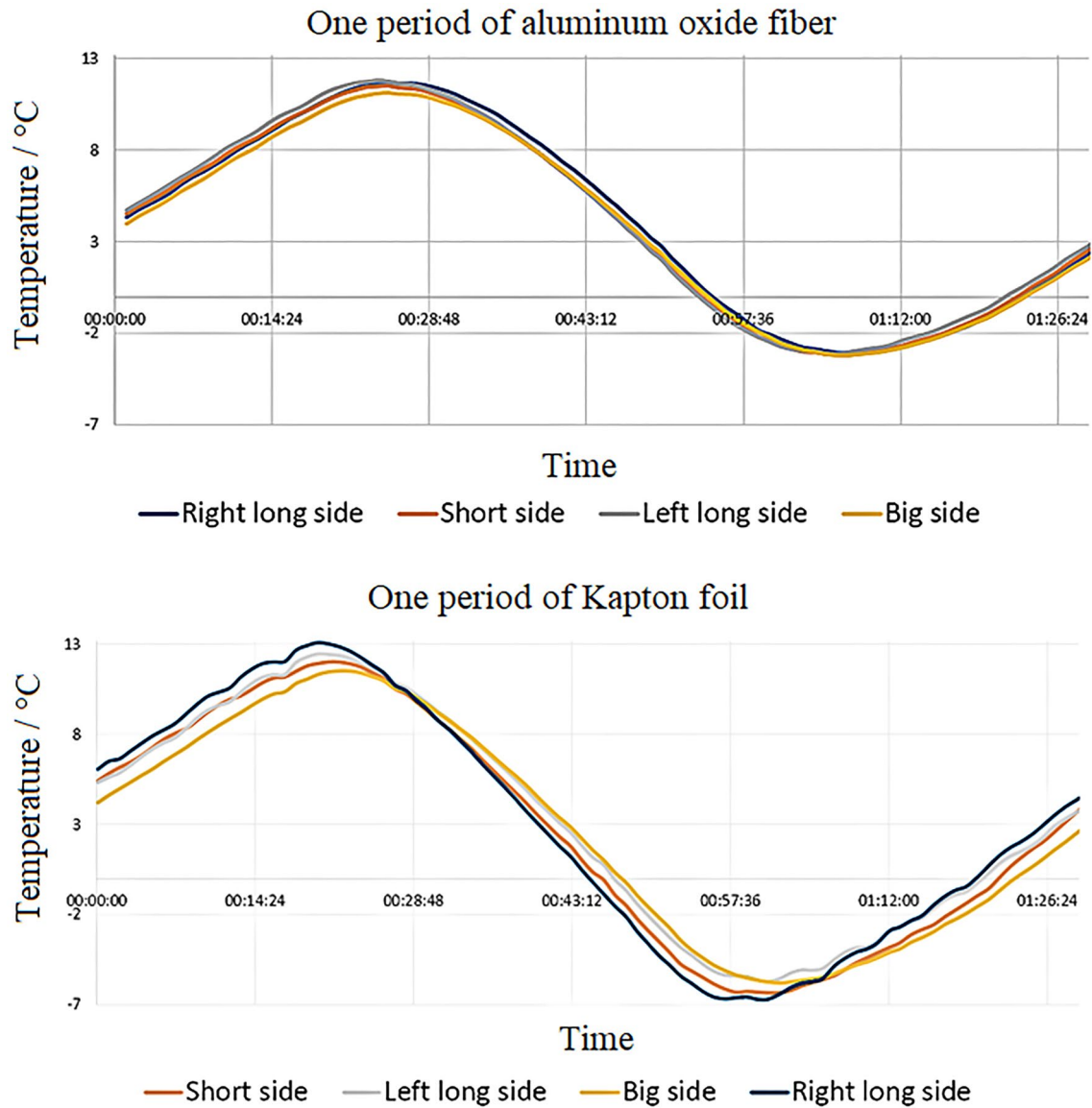
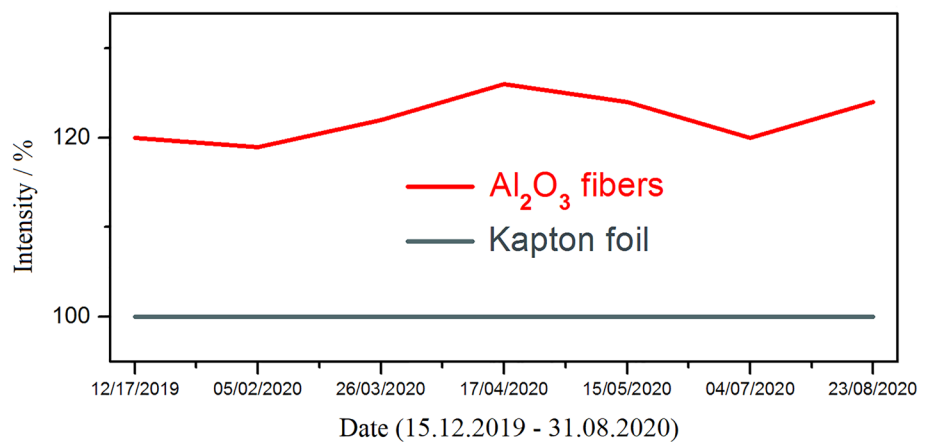


Fig. 7 Temperature fluctuation on the various sides of the batteries

Fig. 8 Thermal insulation ability of Al<sub>2</sub>O<sub>3</sub> fibers correlated to that of Kapton foil



$$\lambda = \left( \frac{T_{\max, \text{Kap}} - T_{\min, \text{Kap}}}{T_{\max, \text{Fib}} - T_{\min, \text{Fib}}} \right) \cdot 100 \quad (1)$$

where  $T_{\max \text{Kap}}$  maximum temperature of Kapton foil,  $T_{\min \text{Kap}}$  minimum temperature of Kapton foil,  $T_{\max \text{Fib}}$  maximum temperature of  $\text{Al}_2\text{O}_3$  fibers,  $T_{\min \text{Fib}}$  minimum temperature of  $\text{Al}_2\text{O}_3$  fibers.

The fibers are aimed to apply as insulation materials at higher temperature ( $> 800$  °C) for protection of e.g., cryogenic tanks. Our ultralight  $\text{Al}_2\text{O}_3$  fibers could retain their fibrillar and porous characters even at  $1500$  °C (Fig. 9). The pure silica aerogels are applicable up to about  $650$  °C, while the commercial bulk  $\text{Al}_2\text{O}_3$  insulation materials generally up to  $1000$  °C. Typical problem of applicability of  $\text{Al}_2\text{O}_3$  above  $1000$  °C is the crystallization of alpha  $\text{Al}_2\text{O}_3$ , which

generally breaks the fibrillar and porous structure. The reason of avoiding the fracture is the use of gel-like precursor system of drawing. The near 3D structure hinders the structural degradation.

The fibers were heated at  $1000$  °C for 48 h to control the long-term load. The fibrous and porous structures were retained (Fig. 10).

The very important parameter of insulation materials is the thermal conductivity. The thermal conductivity of  $\text{Al}_2\text{O}_3$  fibers and various insulation materials of space vehicles are listed in Table 1 [25]. The aerogels or aerogel-based hybrid or composite materials have much lower thermal conductance than polymer foam or fiberglass systems. Moreover, the polymer containing systems can be only used at low temperature, lower than  $150$  °C. The silica aerogels (in MLI

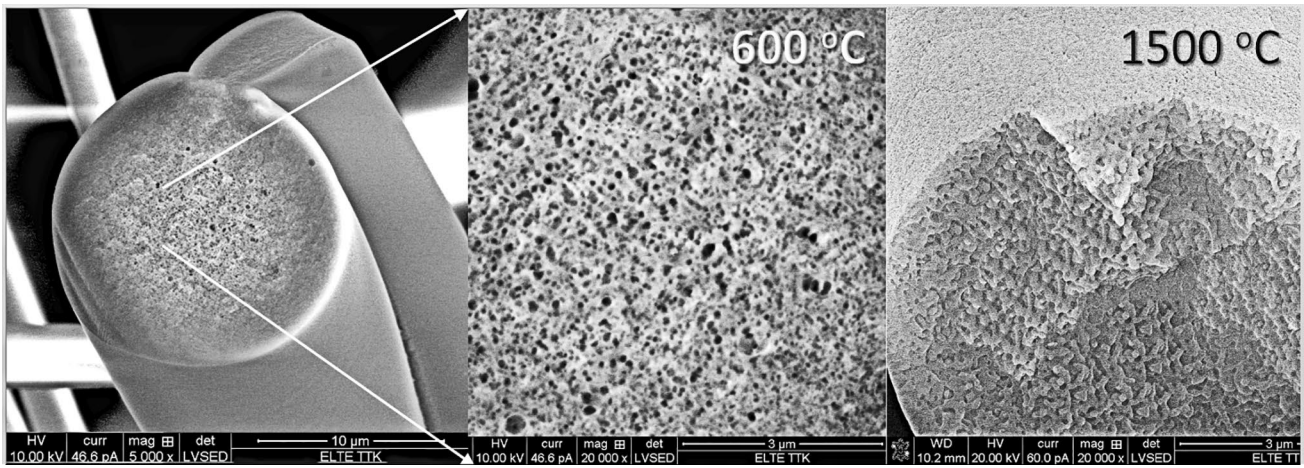


Fig. 9 SEM images for  $\text{Al}_2\text{O}_3$  fibers heat treated at 600 and  $1500$  °C

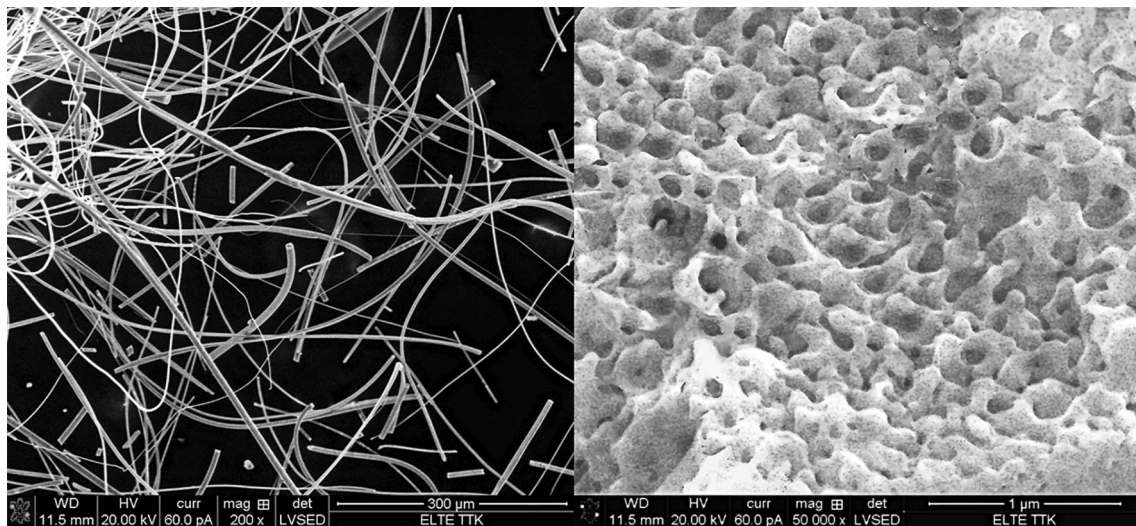


Fig. 10 SEM images for  $\text{Al}_2\text{O}_3$  fibers heat treated at  $1000$  °C for 48 h. The magnifications are 200x and 50000x



**Table 1** Comparison of the ambient thermal conductivity of insulation materials for space vehicles [25]

Materials	Al <sub>2</sub> O <sub>3</sub> fibers	Al <sub>2</sub> O <sub>3</sub> aerogel	Silica aerogel	Polystyrene foam	Polyurethane foam	Fiber glass	Mineral wool	Perlite
Thermal conductivity (mV/mK)	35–37	30–100	20–30	40–200	30–200	40–130	40–150	40–60

and Aspen) possess the best insulation ability, i.e., the lowest thermal conductivity (20–30 mV/mK). The Al<sub>2</sub>O<sub>3</sub> aerogels have a little higher data (30–100 mV/mK). The thermal conductivity data of our Al<sub>2</sub>O<sub>3</sub> fibers (35–37 mV/mK) fits to the data range of aerogels. Our Al<sub>2</sub>O<sub>3</sub> ultralight system retains its fibrous and porous characters up to 1500 °C.

## 4 Conclusions

The main aim of this study was to develop a new low-cost synthesis route to produce ultralight aluminum oxide ceramic fibers for high temperature insulation. In this paper, we mainly focus to control the applicability of fibers by means of test during a launch and in the space conditions. The test results were completed with investigation at high temperature. In the research work, solution techniques (sol–gel and co-precipitation routes) were applied to synthesize spinnable viscous systems. The fibers with best quality possess a homogeneous, porous, amorphous structure. The porous Al<sub>2</sub>O<sub>3</sub> fiber is an extraordinary product of drawing. The porosity of our fibers is kept up to 1500 °C. However, the Al<sub>2</sub>O<sub>3</sub> fibers generally lose their fibrous and porous character above 1000 °C due to the form of  $\alpha$ -Al<sub>2</sub>O<sub>3</sub>. The fiber porosity is 58–65% and the nanopore diameter 40–200 nm. The fibers can be characterized by 0.035–0.037 W·mK<sup>-1</sup> thermal conductivity, excellent heat resistance (up to 1500 °C), and good flexibility.

According to thermo-vacuum and vibration tests, our fibers fill eminently the requirements of satellite launch. In both tests the weight loss is much less than 1%, thus our fibrous samples have obtained the space qualification. In the satellite test, Kapton foil provided the comparison as a typical insulation material of satellite. During the investigation in the space, the insulation character of Al<sub>2</sub>O<sub>3</sub> fibers has slightly changed during near 9 months demonstrating the stability of the fibers even in extreme conditions. The Al<sub>2</sub>O<sub>3</sub> fibrous insulation shows 19–20% smaller temperature fluctuation than Kapton foil. The long-term results of fibers are 12–15 and 20–60% better in maximum and minimum daily temperatures than foil, respectively. However, both systems meet the operating requirements, but the battery covered with Kapton foil can be chargeable in 30–40% shorter time. Our fibrous material could achieve these prosperous results using only in 1 mm layer thickness around the battery. This

layer thickness quarantined the reliable comparison with Kapton foil.

**Acknowledgements** This work was completed in the ELTE Institutional Excellence Program (1783-3/2018/FEKUTSRAT) supported by the Hungarian Ministry of Human Capacities. This work was prepared with the professional support of the Doctoral Student Scholarship Program of the Co-operative Doctoral Program of the Ministry of Innovations and Technology financed from the national Research, Development and Innovation Fund.

**Funding** Open access funding provided by Eötvös Loránd University.

## Declarations

**Conflict of interest** The authors declare the following financial interests/personal relationships which may be considered as potential competing interests. The authors declare the following financial interests/personal relationships which may be considered as potential competing interests.

**Open Access** This article is licensed under a Creative Commons Attribution 4.0 International License, which permits use, sharing, adaptation, distribution and reproduction in any medium or format, as long as you give appropriate credit to the original author(s) and the source, provide a link to the Creative Commons licence, and indicate if changes were made. The images or other third party material in this article are included in the article's Creative Commons licence, unless indicated otherwise in a credit line to the material. If material is not included in the article's Creative Commons licence and your intended use is not permitted by statutory regulation or exceeds the permitted use, you will need to obtain permission directly from the copyright holder. To view a copy of this licence, visit <http://creativecommons.org/licenses/by/4.0/>.

## References

1. NASA, Wings in Orbit. Scientific and Engineering Legacies of the Space Shuttle, pp. 182–199 (2010)
2. NASA, State of the art of small spacecraft technology, chapter 7. Thermal control. NASA <https://www.nasa.gov/smallsat-institute/sst-soa/thermal-control> (2021). Accessed 01 Mar 2022
3. Fischer, M.: Flexure to put NASA thermal insulation technology to work. Space. Safety. Magazine. (2012)
4. Harbaugh, J.: Foam and cork insulation protects deep space rocket from fire and ice. Space Lunch System. NASA online publication: <https://www.nasa.gov/exploration/systems/sls/insulation-protects-sls-from-fire-and-ice> last (2018). Accessed 01 Mar 2022
5. Harbaugh, J.: Thermal insulation protects the space launch system rocket. NASA online publication: <https://www.nasa.gov/exploration/systems/sls/multimedia/tps-on-lvsa.html> last successful (2019). Accessed 01 Mar 2022

6. Tariq, M., Hanif, F., Ashraf, A.: Overview of Nextel™ based structures for space applications. *J. Space. Technol.* **1**, 88–94 (2011). (ISSN 2077–3099)
7. Sedaghat, A., Taheri-Nassaj, E., Naghizadeh, R.: An alumina mat with a nano microstructure prepared by centrifugal spinning method. *J. Non-Cryst Solids* **352**(26–27), 2818–2828 (2006). <https://doi.org/10.1016/j.jnoncrysol.2006.02.068>
8. Venkatesh, R., Chakrabarty, P.K., Siladitya, B., Chatterjee, M., Ganguli, D.: Preparation of alumina fiber mats by a sol-gel spinning technique. *Ceram. Int.* **25**, 539–543 (1999). [https://doi.org/10.1016/S0272-8842\(97\)00092-8](https://doi.org/10.1016/S0272-8842(97)00092-8)
9. Han, C., Li, H., Pu, H., Yu, H., Deng, L., Huang, S., Luo, Y.: Synthesis and characterization of mesoporous alumina and their performances for removing arsenic(V). *J. Chem. Eng.* **217**, 1–9 (2013). <https://doi.org/10.1016/j.cej.2012.11.087>
10. Clauss, B., Schawaller, D.: Modern aspect of ceramic fiber development. *Adv. Sci. Technol.* **50**, 1–8 (2006). <https://doi.org/10.4028/www.scientific.net/AST.50.1>
11. Gumen, V., Ul Haq, A., Illyas, B., Maqsood, A.: High-temperature thermal conductivity of ceramic fibers. *J. Mat. Eng. Perform.* **10**, 475–478 (2001). <https://doi.org/10.1361/105994901770344917>
12. Yoldas, B.E.: Hydrolysis of aluminium alkoxides and bayerite conversion. *J. Appl. Chem. Biotechnol.* **23**, 803–809 (1973). <https://doi.org/10.1002/jctb.5020231103>
13. Maki, T., Sakka, S.: Preparation of alumina fibers by sol-gel method. *J. Non-Cryst. Solids* **100**, 303–308 (1988). [https://doi.org/10.1016/0022-3093\(88\)90037-3](https://doi.org/10.1016/0022-3093(88)90037-3)
14. Sharifi, L., Assa, F., Ajamein, H., Mirhosseini, S.H.: Effect of Voltage and distance on synthesis of boehmite nanofibers with PVP by the electrospinning method. *Int. J. Adv. Sci. Technol.* **98**, 63–74 (2017). <https://doi.org/10.14257/ijast.2017.98.06>
15. Krivoschapkin, P.V., Krivoschapkina, E.F., Dudkin, B.N.: Growth and structure of microscale fibers as precursors of alumina nanofibers. *J. Phy. Chem. Solids* **74**, 991–996 (2013). <https://doi.org/10.1016/j.jpcs.2013.02.021>
16. Jeon-Hee, K.Y., Dong-Heui, K., Heung-Joe, J., Tae-Young, K., Kyung-Hee, P., Jae-Wook, L.: Characterization and application of electrospun alumina nanofibers. *Nanoscale. Res. Lett.* **9**(44), 44–50 (2014). <https://doi.org/10.1186/1556-276X-9-44>
17. Yan, W., Wei, L., Xiuling, J., Dairong, C.: Electrospinning preparation and adsorption properties of mesoporous alumina fibers. *J. Mater. Chem. A* **1**, 10720–10726 (2013). <https://doi.org/10.1039/C3TA10955K>
18. Akiaa, M., Capitanachia, D., Martíneza, M., Hernández, C., de Santiago, B.H., Maob, Y., Lozano, K.: Development and optimization of alumina fine fibers utilizing a centrifugal spinning process. *Microporous. Mesoporous. Mater.* **262**, 175–181 (2018). <https://doi.org/10.1016/j.micromeso.2017.11.039>
19. Zhenfeng, Z., Hui, L., Hongjung, S., Dong, Y.: PEG-directed hydrothermal synthesis of multilayered alumina microfibers with mesoporous structures. *Microporous. Mesoporous. Mater.* **123**, 39–44 (2009). <https://doi.org/10.1016/j.micromeso.2009.03.028>
20. Riley, F.L.: Concise encyclopedia of advanced ceramic materials. Pergamon, Oxford (1991)
21. Sinkó, K., Temesi, O., Ádám, P., Nagy, A.: Process for the production of 100% alumina, porous, fibrous material. *Hungarian Patent P2100158* (2021)
22. Dudás, L., Gschwindt, A.: The Communication and Spectrum Monitoring System of Smog-1 PocketQube Class Satellite. In: Rydosz, A, 21st International Conference on Microwave, Radar and Wireless Communications (MIKON), IEEE (2016)
23. Homepage of satellite project of Budapest University of Technology and Economics, Faculty of Electrical Engineering and Computer Science, Department of Broadband Communications and Electrical Engineering, <https://gnd.bme.hu/smog/#satellite>, Accessed 01 Mar 2022
24. Standard: Criteria for explosive systems and devices on space and launch vehicles (AIAA S-113A-2016)
25. Mital, S. K., Gyekenyesi, J. Z., Arnold, S. M.: Review of current state of the art and key design issues with potential solutions for liquid hydrogen cryogenic storage tank structures for aircraft applications NASA/TM—2006-214346 (2006)

**Publisher's Note** Springer Nature remains neutral with regard to jurisdictional claims in published maps and institutional affiliations.